

Document downloaded from:

<http://hdl.handle.net/10251/160915>

This paper must be cited as:

Duran-Giner, N.; Carlotti, B.; Clementi, C.; Elisei, F.; Encinas Perea, S.; Miranda Alonso, M^Á. (2019). Transient absorption spectroscopic studies on 4-nitroquinoline N-oxide: From femtoseconds to microseconds timescale. *Spectrochimica Acta Part A Molecular and Biomolecular Spectroscopy*. 216:265-272. <https://doi.org/10.1016/j.saa.2019.02.105>

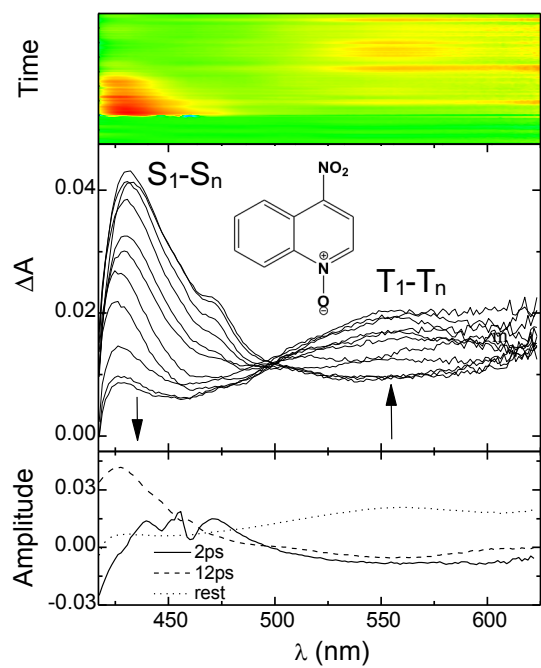


The final publication is available at

<https://doi.org/10.1016/j.saa.2019.02.105>

Copyright Elsevier

Additional Information



The figure shows intersystem crossing within ca. 100 ps from the S_1 to the T_1 excited state of the title compound

Highlights for the MS entitled “Transient Absorption Spectroscopic Studies on 4-Nitroquinoline N-Oxide: from Femtoseconds to Microseconds Timescale”

Singlet to triplet 4-nitroquinoline N-oxide intersystem crossing in femtosecond scale

Nitroquinoline N-oxide radical anion formed via electron transfer with electron donor

Nitroquinoline N-oxide protonated radical formed with electron and proton donors

Singlet and triplet excited states of nitroquinoline N-oxide completely characterized

Transient Absorption Spectroscopic Studies on 4-Nitroquinoline *N*-Oxide: from Femtoseconds to Microseconds Timescale

Neus Duran-Giner,^[a] Benedetta Carlotti,^[b] Catia Clementi,^[b] Fausto Elisei,^[b] Susana Encinas,^{*,[a]} and Miguel A. Miranda,^{*,[a]}

Abstract: The singlet excited state of 4-nitroquinoline *N*-oxide ($^1\text{NQNO}^*$) has been characterized by different spectroscopic techniques, combining transient absorption with steady state and time-resolved emission spectroscopy. The energy of $^1\text{NQNO}^*$ has been established as 255 kJ/mol from the fluorescence spectrum, whereas its lifetime has been found to be 10 ps in the femto-laser flash photolysis (LFP) experiments, where a characteristic S_1-S_n absorption band with maximum centered at 425 nm is observed. In a first stage, the triplet excited state of NQNO ($^3\text{NQNO}^*$) has also been characterized by emission spectroscopy in solid matrix, at low temperature. Thus, from the steady-state phosphorescence spectrum the triplet energy has been estimated as 183 kJ/mol, whereas the setup with time resolution has allowed us to determine the phosphorescence lifetime as 3 ms. Formation of $^3\text{NQNO}^*$ by intersystem crossing in solution at room temperature, has been monitored by femto-LFP, which shows the appearance of a band with maximum at 560 nm (T_1-T_n). It increases with the decreasing intensity of its precursor 425 nm (S_1-S_n) band, giving rise to an isosbestic point at 500 nm. The characterization of $^3\text{NQNO}^*$ has been completed by nano-LFP, using xanthone as photosensitizer and oxygen as well as β -carotene as quenchers. In addition, quenching of $^3\text{NQNO}^*$ by electron donors (DABCO) is also observed in aprotic solvents, leading to the radical anion of NQNO ($\cdot\text{NQNO}$). If there is a proton source in the medium (Et_3N as electron donor or $\text{MeCN}:\text{H}_2\text{O}/4:1$ as solvent system) protonation of the radical anion results in formation of the neutral radical of NQNO ($\cdot\text{NQNOH}$). In general, all processes are slower in protic solvents because of the solvation sphere. Overall, this information provides a deeper insight into the formation and behavior of excited states and radical ionic species derived from the title molecule NQNO.

1. Introduction

Imino *N*-oxides exhibit a rich and complex photochemistry, which has attracted considerable interest since the beginning of the sixties. In particular, heterocyclic *N*-oxides mediate

photoinduced oxidative DNA damage and may act as enzyme-mimics in photochemical oxidations. As they absorb in the near UV or even the visible, it appears worthwhile to investigate biological oxidations based on these compounds.¹⁻³

Specifically, 4-nitroquinoline *N*-oxide (NQNO, Figure 1) is used as a model carcinogen that causes DNA damage. Its mutagenic and carcinogenic properties are linked to its ability to form charge transfer complexes (CT) with DNA.⁴⁻⁶

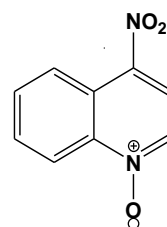


Figure 1. Molecular structure of 4-nitroquinoline *N*-oxide (NQNO).

The excited state dynamics of NQNO (essential to understand its photobiological properties) is partially known, but there are still key aspects that require further investigation. For instance, fluorescence emission spectra in aqueous solution have been reported⁷ but the corresponding excitation spectra are not published; in addition, neither the excited singlet state lifetime nor its energy have been determined.

Although some information on the NQNO triplet excited state ($^3\text{NQNO}^*$) is available, the characterization of this excited state is still incomplete. The phosphorescence emission and excitation spectra have been recorded in organic media at 77 K; the emission with maximum in the 670-710 nm region, is attributed to a π - π transition; it decays with a lifetime of 10 ms.⁸ Furthermore, the triplet energy of NQNO in a methanol:ethanol mixture (1:1 in volume) has been determined as $E_T = 177$ kJ/mol.⁹

In addition, $^3\text{NQNO}^*$ has been investigated in solution by laser flash photolysis (LFP); its transient absorption spectrum in acetonitrile displays a maximum at 560 nm.^{9,10} In benzene the absorption band is centered at 530 nm and has a lifetime of 26 μs .⁹ In buffered aqueous solutions (pH = 7) $^3\text{NQNO}^*$ exhibits maxima at 410 and 590 nm ($\tau = 50$ μs) and appears together with a species peaking at 450 nm ($\tau > 100$ μs), which has been attributed to the NQNO protonated radical ($\text{NQNOH}\cdot$).^{9,11} Moreover, the quantum yields of $^3\text{NQNO}^*$ and $\text{NQNOH}\cdot$ formation have been determined as 0.46 and 0.47; their molar

[a] Drs. N. Durán-Giner, S. Encinas, M. A. Miranda
Chemistry Department/Instituto de Tecnología Química
Universitat Politècnica de València
Avda de los Naranjos s/n, 46022 Valencia, Spain
E-mails: sencinas@qim.upv.es, mmiranda@qim.upv.es

[b] Drs. B. Carlotti, C. Clementi, F. Elisei
Department of Chemistry, Biology and Biotechnology
Università degli Studi di Perugia
Via Elce di Sotto 8, 06123 Perugia, Italy

absorption coefficients are $7600 \text{ dm}^3 \text{ mol}^{-1} \text{ cm}^{-1}$ (at 590 nm) and $13000 \text{ dm}^3 \text{ mol}^{-1} \text{ cm}^{-1}$ (at 450 nm), respectively.¹¹

In the presence of electron donors $^3\text{NQNO}^*$ gives rise to the NQNO radical anion ($\text{NQNO}^{\cdot -}$), whose subsequent protonation results in the formation of $^1\text{NQNOH}$.⁹⁻¹² Both intermediates have been characterized by means of LFP.¹² In the case of $\text{NQNO}^{\cdot -}$ two transient absorption maxima at 490 and 520 nm have been determined,¹³ while in the case of $^1\text{NQNOH}$ its absorption maximum depends on the solvent within the 440-470 nm range.^{9,11} According to infrared spectroscopic studies, together with theoretical calculations,^{12,14} the *N*-oxygen in $\text{NQNO}^{\cdot -}$ is the most suitable protonation site; nevertheless, additional efforts are required for a better mechanistic characterization of the NQNO photophysics.

Hence, the aim of this research is to achieve a complete characterization of the excited state dynamics of NQNO in different media by means of a combination of steady-state and time-resolved emission and absorption spectroscopies, including nano and femtosecond laser flash photolysis. In order to understand the photobiological damage produced by NQNO, special attention is devoted to the study of electron transfer between different donors and $^3\text{NQNO}^*$.

2. Experimental Section

All reagents (NQNO, β -Car, DABCO, Et_3N , naphthalene) were commercially available and used as received from Sigma-Aldrich® without further purification. All organic solvents used were of analytical grade and purchased from Merck®.

The UV/Vis spectra were recorded using a Jasco V-650 spectrophotometer. The experiments in the absorption spectrophotometer were performed on an acetonitrile solution of NQNO in quartz cells of 10 mm x 10 mm dimensions with a maximum capacity of 4 ml. The measurements were made under a nitrogen atmosphere at 22 °C for the 1×10^{-5} M solutions.

The fluorescence experiments were performed on NQNO acetonitrile solutions at a concentration of 1×10^{-5} M. The excitation spectrum was recorded at the 540 nm emission wavelength, while for recording the emission spectrum the excitation maximum at 390 nm was used. The NQNO fluorescence quantum yield (ϕ_{NQNO}) was determined employing naphthalene (NP) as the reference compound ($\phi_{\text{NP}} = 0.1$ in MeCN under N_2)¹⁵ and applying Equation (1).

$$\phi_{\text{NQNO}} = \phi_{\text{NP}} \times A_{\text{NP}} / A_{\text{NQNO}} \times I_{\text{NQNO}} / I_{\text{NP}} \times n_{\text{NQNO}}^2 / n_{\text{NP}}^2 \quad (1)$$

Where *A* is the absorbance at the excitation wavelength, *I* is the area covered by the fluorescence spectrum and *n* is the refractive index of the solvent. The emission measurements were carried out in the range of 320-500 nm. It was not possible to accurately determine the fluorescence lifetime, since the sample decay was shorter than that of the irradiation lamp (~ 1 ns). The steady-state emission spectra were measured using an FP-8500 Jasco spectrofluorometer equipped with a SCE-846 and a xenon 150W lamp. The time-resolved fluorescence measurements were performed using an EasyLife X (Optical Building Blocks) spectrofluorimeter with a Photon Technology International (PTI) nanosecond detector, coupled with LED lamps at different wavelengths and several filters.

The phosphorescence emission experiments were carried out at low temperature (77 K) with sample concentration of 5×10^{-5} M in ethanol (sample absorbances lower than 0.1 u.a.). All the steady-state and time-resolved phosphorescence measurements were recorded in a PTI TM 2/2003 model spectrophotometer equipped with a xenon lamp.

The experimental setup for ultrafast spectroscopic and kinetic measurements (femto-LFP) has been widely used and described elsewhere.¹⁶ Briefly, the 400 nm excitation pulses of ca. 40 fs were generated by an amplified Ti:sapphire laser system (Spectra Physics, Mountain View, CA). The transient absorption setup (Helios, Ultrafast Systems, Sarasota, FL) is characterized by a temporal resolution of ca. 150 fs and spectral resolution of 1.5 nm. Probe pulses for optical measurements were produced by passing a small portion of the 800 nm light through an optical delay line (with a time window of 3200 ps) and focusing it into a 2 mm thick sapphire or CaF_2 window to generate a white-light continuum in the 475–800 nm or 400-625 nm range, respectively, depending on the spectral region of interest. The chirp inside the sample cell was determined by measuring the laser-induced Kerr signal of the solvent. All the measurements were carried out under magic angle conditions, in a 2 mm cell and with an absorbance ranging from 0.3 to 1.0 at 400 nm. The samples were stirred during the measurements to prevent photodegradation. Transient absorption data were analyzed using the Surface Explorer PRO (Ultrafast Systems)¹⁷ which allows us to perform the singular value deconvolution of the 3D surface into principal components (spectra and kinetics) followed by global analysis (giving lifetimes with an error of ca. 10% and decay associated spectra, DAS, of the detected transients).

The nano-LFP experiments were performed under the 355 nm excitation wavelength ($[\text{NQNO}] = 3 \times 10^{-5}$ M), with a pulse duration <10 ns and a power of 15mJ. The 3 mL NQNO solutions were placed in 10x10 mm quartz cuvettes at room temperature and purged with nitrogen or oxygen for 20 min prior to performing the measurements. The absorbance of the samples remained below 0.4. All nanosecond transient absorption spectra were recorded with a Quantel Brilliant pulsed Nd:YAG laser coupled with a mLFP-111 Luzchem miniaturized equipment.

3. Results and Discussion

3.1. Characterization of the NQNO singlet excited state

Figure 2 shows the normalized absorption, fluorescence (F) emission and excitation spectra of NQNO; from their intersection the energy of the excited singlet state ($^1\text{NQNO}^*$) was determined as 255 kJ/mol (470 nm). The fluorescence quantum yield, calculated using naphthalene as the standard, gave a very low value, $\phi_{\text{F}} = 0.001$. The fluorescence lifetime could not be determined with the available equipment due to insufficient time resolution (ca. 1 ns).

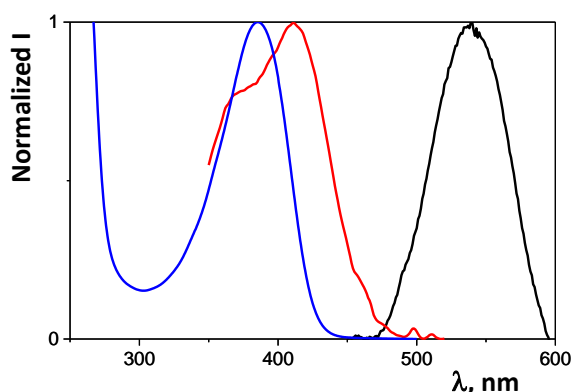


Figure 2. Comparison of NQNO absorption (blue) fluorescence excitation ($\lambda_{em} = 540$ nm) and fluorescence emission ($\lambda_{ex} = 390$ nm) (black) spectra, normalized to their maxima (MeCN / N_2 / 298 K).

The NQNO transient absorption spectrum was characterized in the ultrafast mode, using LFP in the femtosecond scale (femto-LFP). The statistical elaboration of the results provided three components (Table 1): i) vibrational cooling (VC) with a lifetime of approximately 2 ps; ii) singlet excited state absorption (S_1-S_n) with a lifetime of approximately 10 ps; iii) triplet excited state absorption (T_1-T_n) with a very long lifetime that could not be measured in this timescale and matched the triplet band found by LFP in the nanoseconds range (see below).

Table 1. Values obtained after global analysis of the NQNO data generated by femto-LFP using two different crystals ($\lambda_{ex} = 400$ nm / MeCN / 298 K).

Compound	Crystal	λ (nm)	τ (ps)	Assignment
NQNO/MeCN	CaF ₂	460(+)	2	VC
		430(+),560(-)	12	S_1-S_n
		560(+)	rest	T_1-T_n
NQNO/MeCN	Sapphire	460(+)	1.6	VC
		430(+),560(-)	10	S_1-S_n
		560(+)	rest	T_1-T_n

The S_1-S_n absorption band at 430 nm decreased simultaneously with the increasing T_1-T_n absorption band at 560 nm, and an isosbestic point appeared at 500 nm (Figure 3). This process was associated with intersystem crossing leading to formation of $^3NQNO^*$ from $^1NQNO^*$ and confirmed the transient species assignment.

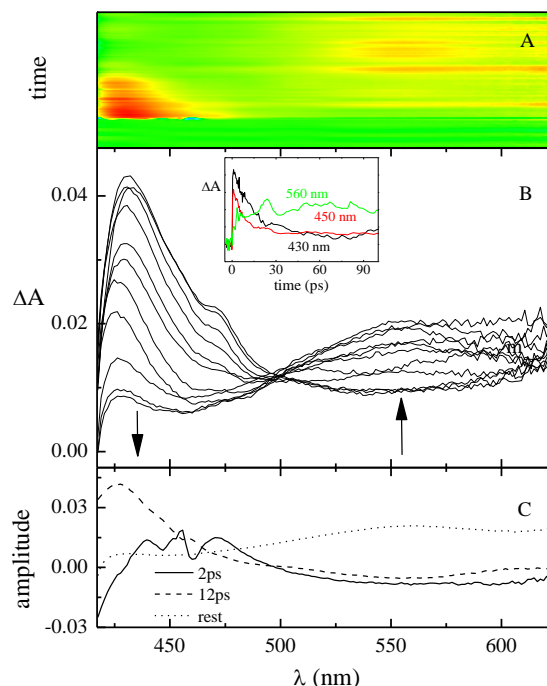
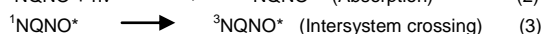


Figure 3. Data obtained by NQNO femto-LFP in MeCN. A: Contour plot of the data. B: Monitoring of transient absorption spectra at different times (0.6, 1, 1.6, 2.6, 4.4, 6, 10, 14, 19, 39 and 115 ps). Inset: Kinetic decays at the most representative wavelengths. C: Transient absorption spectra of the main components and their lifetimes ($\lambda_{ex} = 400$ nm / CaF₂ / MeCN / 298 K).

Thus, NQNO excitation leads to the singlet excited state, which is converted into the triplet excited state (Equations 2 and 3).



The short lifetime of the S_1-S_n absorption band (~ 10 ps), is in agreement with the fact that the fluorescence lifetime could not be determined by our available emission instrumentation.

3.2. Characterization of the NQNO triplet excited state

As shown in Figure 4, the NQNO phosphorescence (P) spectrum was recorded under low temperature in solid matrix. From the position of the emission band, the $^3NQNO^*$ energy was estimated at $E_T = 655$ nm (183 kJ/mol). By monitoring the disappearance of the signal at the phosphorescence maximum (inset of Figure 4) a triplet lifetime of $\tau = 3$ ms was obtained.

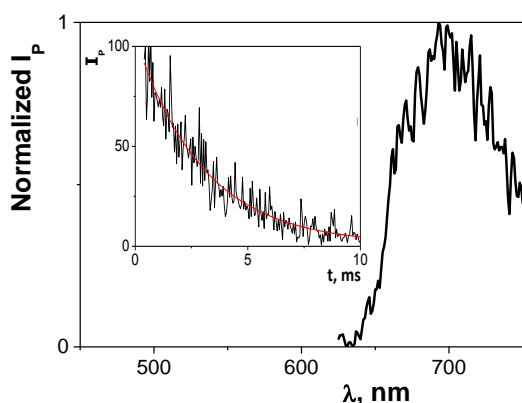


Figure 4. NQNO low-temperature phosphorescence spectrum ($\lambda_{\text{ex}} = 390$ nm) normalized to the maximum. Inset: Phosphorescence decay ($\lambda_{\text{em}} = 690$ nm / EtOH / 77 K).

In order to characterize the NQNO triplet excited state in solution, nanosecond LFP (nano-LFP) was used. As shown in Figure 5, a transient spectrum with absorption maximum at 560 nm was obtained, which was attributed to the NQNO triplet-triplet (T_1 - T_n) absorption according to the literature.¹⁰

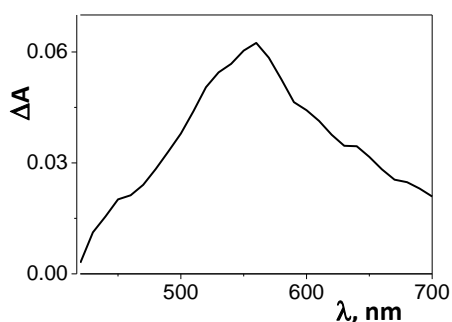


Figure 5. NQNO nano-LFP T_1 - T_n absorption spectrum recorded at 0.5 μs after the laser pulse (MeCN / $\lambda_{\text{ex}} = 355$ nm / N_2).

As the triplet excited state energy was known ($E_T = 183$ kJ/mol, see above), the assignment was confirmed by interaction with quenchers such as β -carotene (βCAR) and molecular oxygen.

The intersystem crossing quantum yield of βCAR is very small. In addition, the resulting triplet state exhibits a low energy level ($^3\beta\text{CAR}^* \sim 64$ kJ/mol) and a very narrow shape for the T_1 - T_n band with maximum at 510 nm. When the nano-LFP experiment was performed on the NQNO: βCAR 1:2 mixture, under NQNO irradiation, the transient absorption spectrum T_1 - T_n of $^3\beta\text{CAR}^*$ was obtained as the main species after 3 μs (Figure 6A), which would agree with an exergonic energy transfer.

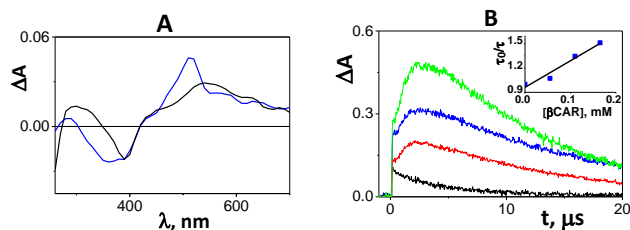


Figure 6. A: Normalized transient absorption spectra by nano-LFP ($\lambda_{\text{ex}} = 355$ nm) of NQNO (black) and NQNO: βCAR 1:2 (blue) 3 μs after the laser pulse. B: Kinetics of the $^3\text{NQNO}^*$ deactivation and $^3\beta\text{CAR}^*$ formation at different concentrations of βCAR (NQNO: βCAR 1:0 black, 1:1 red, 1:2 blue, 1:3 green) and $[\text{NQNO}] = 5.5 \times 10^{-5}$ M ($\lambda_{\text{ex}} = 355$ nm, $\lambda_{\text{obs}} = 510$ nm, MeCN, N_2). Inset: Stern-Volmer plot of $^3\text{NQNO}^*$ lifetime ratio vs βCAR concentration (being τ_0 and τ the $^3\text{NQNO}^*$ lifetimes in the absence and in the presence of different concentrations of βCAR).

When the kinetic traces were compared at the $^3\beta\text{CAR}^*$ maximum (Figure 6B) for different NQNO/ βCAR mixtures, keeping the NQNO concentration constant, both the $^3\beta\text{CAR}^*$ formation rate as its top absorption increased. The rate constant (k_q) of $^3\text{NQNO}^*$ quenching by βCAR was obtained using the Stern-Volmer equation (Figure 6B, inset); the k_q value was $(4.4 \pm 0.8) \times 10^8 \text{ M}^{-1}\text{s}^{-1}$.

The ability of molecular oxygen ($^3\text{O}_2$) as a good triplet excited state quencher ($E_T = 92$ kJ/mol) was used to confirm the $^3\text{NQNO}^*$ assignment. For this purpose, two NQNO isoabsorptive solutions at the excitation wavelength ($[\text{NQNO}] = 5.5 \times 10^{-5}$ M) were exposed to air ($[\text{O}_2] = 1.9 \times 10^{-3}$ M, in MeCN)¹⁸ or purged with nitrogen ($[\text{O}_2] = 0$ M). After LFP measurements ($\lambda_{\text{ex}} = 355$ nm), a significant decrease of the signal at 560 nm, corresponding to $^3\text{NQNO}^*$, was observed when oxygen was present (data not shown). Therefore, the NQNO excited triplet species was disabled by the presence of oxygen in the medium. Thus, the $^3\text{NQNO}^*$ intermolecular quenching constant by $^3\text{O}_2$ was calculated, using the Stern-Volmer relationship, with a value of $k_q = (1.4 \pm 0.1) \times 10^9 \text{ M}^{-1}\text{s}^{-1}$.

3.3. NQNO excited states reactivity in the presence of electron donors

Nanosecond LFP experiments were performed in MeCN and in MeCN:H₂O 4:1 mixture, using $[\text{NQNO}] = 5.5 \times 10^{-5}$ M and 4.0×10^{-5} M, respectively, in order to have isoabsorptive solutions at the excitation wavelength (355 nm). In addition, the use of diazabicyclooctane (DABCO) and triethylamine (Et_3N) as electron or electron plus proton donor, respectively, was studied in both protic and aprotic solvents.

First, the NQNO transient absorption spectra (Figure 7) were recorded at different times, and also the corresponding kinetics at the absorption maxima were registered. In an aprotic medium the maximum observed at 560 nm was assigned to $^3\text{NQNO}^*$ (Figure 7A) and it showed a lifetime of 6 μs . This triplet excited species decayed without giving rise to any other species.

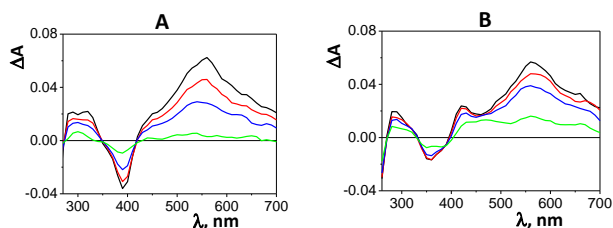


Figure 7. Nano-LFP transient absorption spectra of NQNO in different solvents and recorded at different times after de laser pulse (0.5 μ s black, 1.4 μ s red, 3 μ s blue, 14.3 μ s green). A: MeCN B: MeCN:H₂O 4:1. Isoabsorptive solutions at the 355 nm excitation wavelength in a nitrogen atmosphere.

Conversely, in the protic solvent (Figure 7B), the ³NQNO* transient with maximum at 560 nm and a lifetime of approximately 8 μ s decayed giving rise to a new species. In this sense, at longer times a residual signal appeared at the 420-660 nm range exhibiting a longer lifetime of 25 μ s. This species would result from the interaction between the triplet and the protic solvent and could correspond to the protonated radical ([•]NQNOH). The T₁-T_n absorption maximum of this new species would be fully consistent with the residual signal obtained, as described in the literature.^{9,11}

In both media, the negative band appearing in LFP (peaking around 360-390 nm) also decreased with time. This fact could be due to the UV steady-state absorption associated with the reversible (A) or partially irreversible (B) NQNO depletion in its ground state.

Furthermore, the nanosecond LFP behavior of NQNO was first analyzed in the presence of an electron donor (DABCO) into the aprotic solvent acetonitrile. In this medium a new transient species with absorption maximum at 500 nm was obtained (Figure 8A) and it decayed with a lifetime of 8 μ s. This species was assigned as the NQNO radical anion (NQNO^{•-}), whose formation could be explained according to the process shown in Equation (4).



In this context, considering the initial times (below 2 μ s) after the laser pulse an intersection could be observed in the spectra of Figure 8A. This suggests that NQNO^{•-} would come from ³NQNO*.

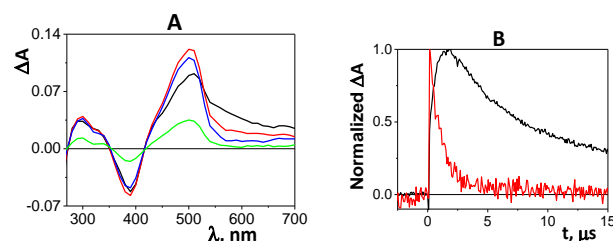


Figure 8. NQNO LFP in the presence of DABCO (1:2 molar relationship between NQNO and DABCO) ($\lambda_{\text{ex}} = 355 \text{ nm} / \text{MeCN} / \text{N}_2$). A: Transient absorption spectra at different times after the laser pulse (0.5 μ s black, 1.4 μ s red, 3 μ s blue, 14.3 μ s green). B: Comparative kinetics of the ³NQNO* decay ($\lambda_{\text{obs}} = 580 \text{ nm}$, red line) and [•]NQNO formation ($\lambda_{\text{obs}} = 500 \text{ nm}$, black line).

Similarly, due to the fact that the NQNO triplet excited state ($\tau = 0.9 \mu$ s at 580 nm) decayed concomitantly with the radical anion formation ($\tau = 0.8 \mu$ s at 500 nm) (as shown in Figure 8B), the previous hypothesis could be confirmed. In addition, a progressive shortening of the N-oxide excited triplet lifetime (Figure 9A) was observed when the NQNO:DABCO ratio was increased. As a result, a quenching rate constant was calculated following the Stern-Volmer equation with a value of $k_q = (7.8 \pm 0.8) \times 10^9 \text{ M}^{-1} \text{ s}^{-1}$ (Figure 9B). This quenching rate constant is due to the electron transfer interaction between ³NQNO* and ground-state DABCO.

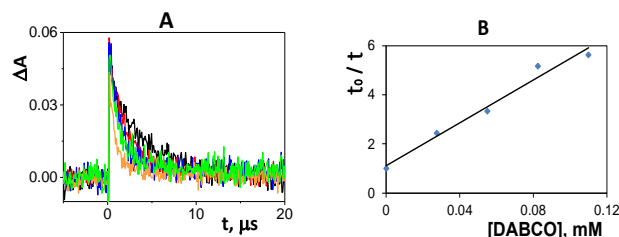


Figure 9. NQNO LFP in the presence of DABCO ($\lambda_{\text{ex}} = 355 \text{ nm} / \text{MeCN} / \text{N}_2$). A: ³NQNO* decay kinetics at 600 nm of different NQNO:DABCO mixtures (1:0k black, 1:0.5 red, 1:1 blue, 1:1.5 green, 1:2 orange). B: Stern-Volmer plot of ³NQNO* lifetime ratio vs DABCO concentration (being τ_0 and τ the ³NQNO* lifetime in the absence and in the presence of different concentrations of DABCO).

Secondly, NQNO acetonitrile solutions were analyzed in the presence of the electron plus proton donor triethylamine (Et₃N). In this environment, the appearance of an isosbestic point at 530 nm was clearly observed in the spectra at different times after the laser pulse (Figure 10A). This crossing point indicates that a different species with maximum at 490 nm is coming from the known ³NQNO* species. Furthermore, the similar lifetimes obtained for the excited NQNO triplet decay ($\tau = 1.7 \mu$ s at 560 nm) and the new species formation ($\tau = 1.4 \mu$ s at 460 nm) (Figure 10B) are supporting the hypothesis that the first species could be the precursor of the second one. The electron transfer interaction between ³NQNO* and the electron plus proton donor Et₃N in its ground state is shown in Equation (5).



The new species exhibited an absorption maximum at 490 nm and a lifetime of $\tau = 25 \mu$ s and was assigned to the NQNO protonated radical ([•]NQNOH). It would result from the electron transfer reaction between ³NQNO* and ground-state Et₃N according to Equation 5.

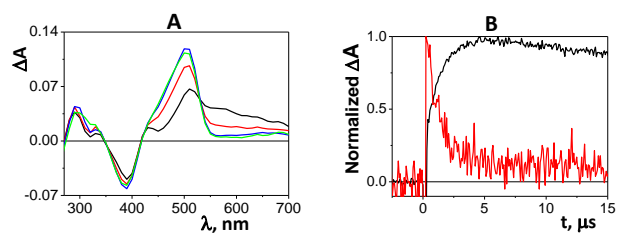


Figure 10. NQNO LFP data in the presence of Et₃N (1:15 NQNO:Et₃N ratio) ($\lambda_{\text{ex}} = 355 \text{ nm} / \text{MeCN} / \text{N}_2$). A: Transient absorption spectra at different times after the laser pulse (0.5 μ s black, 1.4 μ s red, 3 μ s blue, 14.3 μ s green). B:

Kinetics comparison between the $^3\text{NQNO}^*$ decay at 560 nm (red) and the NQNO protonated radical formation at 460 nm (black).

Going further, several NQNO:Et₃N mixtures with different Et₃N proportions were analyzed by using nanosecond LFP measurements (Figure 11A). In the same way as explained above, the NQNO excited triplet decay and the protonated radical formation lifetimes were calculated. The results consisted of a progressive $^3\text{NQNO}^*$ lifetime shortening and then, a quenching constant was calculated, through the Stern-Volmer linear fit shown in Figure 11B, with a value of $k_q = (8.8 \pm 0.8) \times 10^8 \text{ M}^{-1}\text{s}^{-1}$.

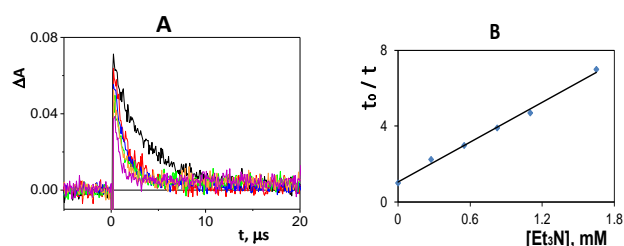


Figure 11. A: $^3\text{NQNO}^*$ decay kinetics at 560 nm of different NQNO:Et₃N mixtures (1:0 black, 1:5 red, 1:10 blue, 1:15 green, 1:20 orange and 1:30 purple) ($\lambda_{\text{ex}} = 355 \text{ nm} / \text{MeCN} / \text{N}_2$). B: Stern-Volmer plot of $^3\text{NQNO}^*$ lifetime ratio vs Et₃N concentration (being τ_0 and τ the $^3\text{NQNO}^*$ lifetime in the absence and in the presence of different concentrations of Et₃N).

With the purpose of gaining further insight into the NQNO photophysical behavior in different media, nanosecond LFP measurements were undertaken on NQNO in the presence of different concentrations of DABCO and in a protic medium like the MeCN:H₂O 4:1 mixture. Under these conditions, when the transient absorption spectrum was recorded an isosbestic point at 500 nm appeared again as it is shown in Figure 12A. This could be indicating that the species in formation (with a maximum at 460 nm) assigned to the NQNO protonated radical arises from $^3\text{NQNO}^*$ (with a maximum at 560 nm). What is confirmed by calculating the $^3\text{NQNO}^*$ decay time ($\tau = 2.7 \mu\text{s}$) and the $^1\text{NQNOH}$ formation time ($\tau = 2.5 \mu\text{s}$) and obtaining very close values (Figure 12B).

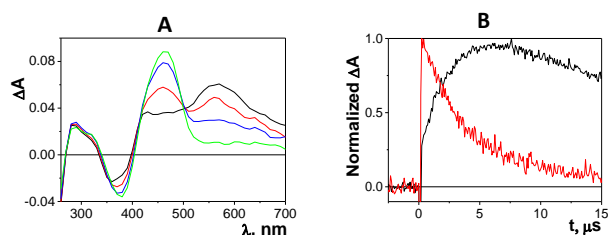
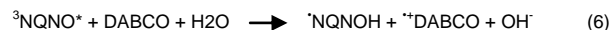


Figure 12. NQNO LFP in the presence of DABCO (1:5 NQNO:DABCO molar ratio) ($\lambda_{\text{ex}} = 355 \text{ nm} / \text{MeCN:H}_2\text{O} 4:1 / \text{N}_2$). A: Transient absorption spectra at different times after the laser pulse (0.5 μs black, 1.4 μs red, 3 μs blue, 8.5 μs green). B: Kinetics comparison between the $^3\text{NQNO}^*$ decay at 560 nm (red) and the NQNO protonated radical formation at 460 nm (black).

On the other hand, when increasing concentrations of DABCO were added to the NQNO:DABCO mixtures the $^3\text{NQNO}^*$ deactivation lifetime was shortened (Figure 13A). Concomitantly, the protonated radical species formation rate

was faster, together with an increase in its yield (Figure 13B). The $^3\text{NQNO}^*$ and $^1\text{NQNOH}$ kinetics were monitored at their corresponding absorption maxima. Considering all these results, a proton-coupled electron transfer process could be envisaged according to Equation (6).



Then, a $^3\text{NQNO}^*$ quenching constant was calculated by means of the Stern-Volmer linear fit (Figure 13C), and a value of $k_q = (1.02 \pm 0.06) \times 10^9 \text{ M}^{-1}\text{s}^{-1}$ was obtained.

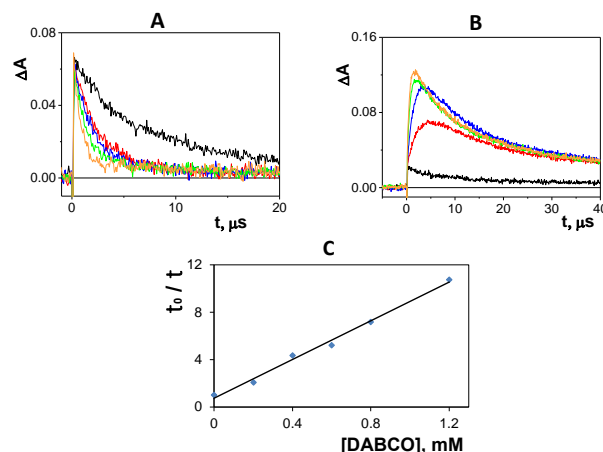


Figure 13. Kinetics comparison by using LFP of different NQNO:DABCO mixtures at different molar ratios (1:0 black, 1:5 red, 1:10 blue, 1:15 green and 1:20 orange) ($\lambda_{\text{ex}} = 355 \text{ nm} / \text{MeCN:H}_2\text{O} 4:1 / \text{N}_2$). A: $^3\text{NQNO}^*$ decay observed at 560 nm. B: $^1\text{NQNOH}$ formation and decay observed at 460 nm. C: Stern-Volmer plot of $^3\text{NQNO}^*$ lifetime ratio vs DABCO concentration (being τ_0 and τ the $^3\text{NQNO}^*$ lifetime in the absence and in the presence of different concentrations of DABCO).

Finally and in the same way as explained before, nanosecond LFP measurements were performed on NQNO in the presence of different concentrations of Et₃N and in the aqueous medium. In this case, an isosbestic point was found again around 500 nm when the transient absorption spectra were recorded at different times after the laser pulse (Figure 14A). This finding indicates that $^3\text{NQNO}^*$ is converted into the proposed species $^1\text{NQNOH}$ and was confirmed by measuring the decay and formation times of the corresponding species (Figure 14B) and obtaining the same result.

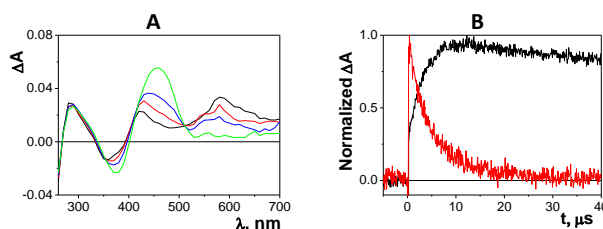


Figure 14. NQNO LFP in the presence of Et₃N (1:15 NQNO:Et₃N molar ratio) ($\lambda_{\text{ex}} = 355 \text{ nm} / \text{MeCN:H}_2\text{O} 4:1 / \text{N}_2$). A: Transient absorption spectra at different times after the laser pulse (0.5 μs black, 1.4 μs red, 3 μs blue, 14.3 μs green). B: Kinetics comparison between $^3\text{NQNO}^*$ decay observed at 560 nm (red) and $^1\text{NQNOH}$ formation observed at 460 nm (black).

Under these new conditions, once the NQNO radical anion is formed from ${}^3\text{NQNO}^*$ it would take protons from both, the solvent and the donor (equation 4), being its formation much faster.

As in the preceding cases, the photophysical interaction between ${}^3\text{NQNO}^*$ and the electron and/or proton donor was measured through an intermolecular quenching constant. In the current case, the obtained value was $k_q = (2.8 \pm 0.8) \times 10^8 \text{ M}^{-1}\text{s}^{-1}$ as resulting from the Stern-Volmer linear fit (Figure 15B). The plot was obtained from the values of the ${}^1\text{NQNOH}$ rising times that were shortened with increasing amounts of Et_3N together with a larger quantity of NQNO protonated radical generated (Figure 15A).

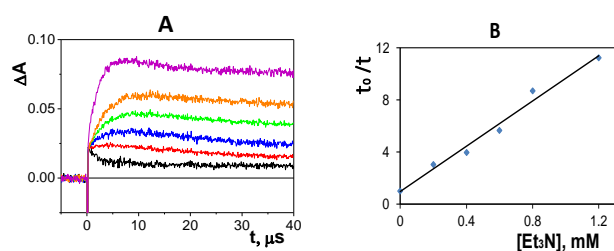


Figure 15. A: ${}^1\text{NQNOH}$ formation kinetics obtained by NQNO LFP in the presence of Et_3N at different NQNO: Et_3N molar ratios (1:0 black, 1:5 red, 1:10 blue, 1:15 green, 1:20 orange, 1:30 purple) ($\lambda_{\text{ex}} = 355 \text{ nm}$ / $\text{MeCN}:\text{H}_2\text{O}$ 4:1 / N_2 / $\lambda_{\text{obs}} = 450 \text{ nm}$). B: Stern-Volmer plot of ${}^1\text{NQNOH}$ rising time ratio vs Et_3N concentration (being τ_0 and τ the ${}^1\text{NQNOH}$ formation time in the absence and in the presence of different concentrations of Et_3N).

4. Conclusions

The singlet excited state of 4-nitroquinoline *N*-oxide (${}^1\text{NQNO}^*$) has been characterized by different techniques. Thus, from the steady-state fluorescence spectrum, it has been possible to determine its energy (255 kJ/mol). In addition, femto-LFP has allowed us to register the $\text{S}_1\text{-S}_n$ absorption spectrum (with maximum at 430 nm and lifetime of 10 ps). The singlet characterization data are shown in Table 2.

Table 2. Photophysical data for NQNO in MeCN.

Absorption		Emission		E, kJ/mol
λ , nm	τ , ps	λ , nm	τ , ns	
430 ^[a]	10 ^[a]	470 ^[a]	-	255 ^[a]
550 ^[b]	6x10 ⁶ ^[b]	655 ^[b]	3x10 ⁶ ^{[b][c]}	183 ^[b]

[a] Singlet excited state data. [b] Triplet excited state data. [c] In solid ethanol matrix at 77K.

Similarly, the triplet excited state of 4-nitroquinoline *N*-oxide (${}^3\text{NQNO}^*$) has been characterized by emission spectroscopy in solid matrix, at low temperature; in this way, the triplet energy has been estimated as 183 kJ/mol from the phosphorescence spectrum, and the emission lifetime has been determined as 3 ms (Table 2). Formation of ${}^3\text{NQNO}^*$ by intersystem crossing from its precursor ${}^1\text{NQNO}^*$ has been evidenced by femto-LFP (as shown by the isosbestic point in Figure 3).

Then, the reactivity of ${}^3\text{NQNO}^*$ under different conditions has been investigated by nano-LFP. As expected for a triplet excited state, it is quenched by oxygen ($k_q = (1.4 \pm 0.1) \times 10^9 \text{ M}^{-1}\text{s}^{-1}$) and β -carotene ($k_q = (3.3 \pm 0.8) \times 10^9 \text{ M}^{-1}\text{s}^{-1}$). Moreover, xanthone photosensitization of ${}^3\text{NQNO}^*$ ($k_q = 4.2 \times 10^{10} \text{ M}^{-1}\text{s}^{-1}$) was demonstrated. In the presence of electron donors (such as DABCO) in aprotic solvents (MeCN), electron transfer occurs to give the radical anion (${}^3\text{NQNO}^{\cdot-}$). Conversely, if proton donors are present in the medium, arising either from a reagent (Et_3N) or from the solvent ($\text{MeCN}:\text{H}_2\text{O}$ 4:1), the protonated radical of NQNO (${}^1\text{NQNOH}$) is produced (Table 3).

Table 3. Excited state species and data for NQNO reactivity in different media

Without additional donors		In the presence of DABCO		In the presence of Et_3N	
Aprotic solvent	Protic solvent	Aprotic solvent	Protic solvent	Aprotic solvent	Protic solvent
${}^3\text{NQNO}^*$ 560nm 6 μs	${}^3\text{NQNO}^*$ 560nm 8 μs	${}^3\text{NQNO}^*$ 560 nm 1.5 μs	${}^3\text{NQNO}^*$ 560 nm >5 μs	${}^3\text{NQNO}^*$ 560 nm 1.5 μs	${}^3\text{NQNO}^*$ 560 nm >5 μs
	${}^1\text{NQNOH}$ 460 nm 25 μs	${}^1\text{NQNO}$ 500nm 8 μs	${}^1\text{NQNOH}$ 460nm 8 μs	${}^1\text{NQNOH}$ 490nm 25 μs	${}^1\text{NQNOH}$ 460nm 1ms
		$k_q^{[a]}$ 8x10 ⁹ M ⁻¹ s ⁻¹	$k_q^{[a]}$ 1x10 ⁹ M ⁻¹ s ⁻¹	$k_q^{[a]}$ 9x10 ⁸ M ⁻¹ s ⁻¹	$k_q^{[a]}$ 3x10 ⁸ M ⁻¹ s ⁻¹

[a] Excited state quenching rate constant

It is worth pointing out that in protic solvents all processes are retarded, probably because of the solvation sphere. Hence, all transient species generated in protic media have typically longer lifetimes and slower decays. Besides, the electron transfer rate constants are lower with Et_3N than with DABCO, which is attributed to the relative oxidation potentials; moreover, the NQNO protonated radical formed in the presence of DABCO lives shorter than when the same species is produced in the presence of Et_3N (see Table 3).

Acknowledgements

The work was financially supported by the Regional Government of Generalitat Valenciana (PROMETEO/2017/075) as well as the Spanish Government Science Department with the CTQ-2016-78875-P and CTQ-2009-13699 projects and the N. D.-G. fellowship (BES-2010-035875). BC, CC and FE acknowledge MIUR and the University of Perugia for financial support to the project AMIS, through the program "Dipartimenti di Eccellenza – 2018-2022".

Keywords: transient absorption spectroscopy • heterocyclic amines • femtosecond laser flash photolysis • electron transfer • 4-nitroquinoline *N*-oxide

References

- [1] (a) T. Fuchs, K. S. Gates, J.-T. Hwang, M. M. Greenberg, *Chem. Res. Toxicol.* **1999**, *12*, 1190-1194; (b) J. S. Daniels, K. S. Gates, *J. Am. Chem. Soc.* **1996**, *118*, 3380-3385.
- [2] D. M. Jerina, D. R. Boyd, J. W. Daly, *Tetrahedron Lett.* **1970**, *11*, 457-460.
- [3] A. Albin, M. Alpegiani, *Chem. Rev.* **1984**, *84*, 43-71.
- [4] T. Nunoshiba, B. Demple, *Cancer Res.* **1993**, *53*, 3250-3252.
- [5] W. Nakahara, F. Fukuoka, T. Sugimura, *Gan* **1957**, *48*, 129-137.
- [6] (a) S. A. Winkle, I. J. Tinoco, *Biochemistry* **1978**, *17*, 1352-1356; (b) J. S. Paul, P. O. B. Jr. Montgomery, B. Louis, *Cancer Res.* **1971**, *31*, 413-419; (c) M. Nagao, T. Sugimura, *Cancer Res.* **1972**, *32*, 2369-2375.
- [7] Z. Sheng, Q. Song, F. Gao, X. Zhou, J. Li, J. Dai, H. Sun, Q. Li, S. Yu, X. Ma, *Res. Chem. Intermed.* **2000**, *26*, 715-725.
- [8] (a) M. Yamakawa, T. Kubota, Y. Mizuno, *Spectrochim. Acta. Part A* **1974**, *30*, 2103-2119; (b) T. Kubota, M. Yamakawa, Y. Mizuno, *Bull. Chem. Soc. Japan* **1972**, *45*, 3282-3286.
- [9] K. Kasama, A. Takematsu, S. Yamamoto, S. Arai, *J. Phys. Chem.* **1984**, *88*, 4918-4921.
- [10] S. D. Choudhury, S. Basu, *J. Phys. Chem. B* **2006**, *110*, 8850-8855.
- [11] H. Seki, A. Takematsu, S. Arai, *J. Phys. Chem.* **1987**, *91*, 176-179.
- [12] X. Shi, M. S. Platz, *J. Phys. Chem. A* **2004**, *108*, 4385-4390.
- [13] K. Ezumi, T. Kubota, H. Miyazaki, M. Yamakawa, *J. Phys. Chem.* **1976**, *80*, 980-988.
- [14] J. S. Daniels, K. S. Gates, C. Tronche, M. M. Greenberg, *Chem. Res. Toxicol.* **1998**, *11*, 1254-1257.
- [15] F. Bosca, S. Encinas, P. F. Heelis, M. A. Miranda, *Chem. Res. Toxicol.* **1997**, *10*, 820-827.
- [16] (a) B. Carlotti, A. Cesaretti, C. G. Fortuna, A. Spalletti, F. Elisei, *Phys. Chem. Chem. Phys.* **2015**, *17*, 1877-1882; (b) A. Cesaretti, B. Carlotti, P. L. Gentili, C. Clementi, R. Germani, F. Elisei, *J. Phys. Chem. B*, **2014**, *118*, 8601-8613; (c) B. Carlotti, A. Cesaretti, F. Elisei, *Phys. Chem. Chem. Phys.* **2012**, *14*, 823-834.
- [17] (a) G. H. Golub, C. F. V. Loan, *Matrix Computations* **1996**; (b) G. Strang, *Introduction to linear algebra*, Wellesley-Cambridge Press, Wellesley, MA, **1998**.
- [18] M. Montalti, A. Credi, L. Prodi, M. T. Gandolfi, *Handbook of Photochemistry*, third edition, CRC Press, Taylor & Francis, **2006**.